

Control of open quantum systems: Case study of the central spin model

Christian Arenz¹, Giulia Gualdi² and Daniel Burgarth¹

¹ Department of Mathematics and Physics, Aberystwyth University, Penglais Campus, SY23 2BZ Aberystwyth, Wales, United Kingdom

² Dipartimento di Fisica ed Astronomia, Università di Firenze, Via Sansone 1, Sesto Fiorentino 50019 Italy; QSTAR, Largo Enrico Fermi 2, 50125 Firenze, Italy

Abstract. We study the controllability of a central spin guided by a classical field and interacting with a spin bath, showing that the central spin is fully controllable independently of the number of bath spins. Additionally we find that for unequal system-bath couplings even the bath becomes controllable by acting on the central spin alone. We then analyze numerically how the time to implement gates on the central spin scales with the number of bath spins and conjecture that for equal system-bath couplings it reaches a saturation value. We provide evidence that sometimes noise can be effectively suppressed through control.

1. Introduction

The last decades have witnessed a spectacular technological progress to the extent that now the implementation of high-fidelity quantum technologies can be thought of as a goal belonging to the not-so-distant future. However the loss of quantum coherence due to the unavoidable interaction of a quantum system with its surrounding environment [1], i.e. decoherence, represents the major obstacle on the way beyond proof-of-concept experiments towards real-life functioning implementations.

On the one hand the quest for a fundamental understanding of the sources and mechanisms of decoherence attracts substantial research effort, while on the other the development of strategies to minimize its detrimental effect in view of practical applications is also a major research focus. Although distinct these two research lines are deeply intertwined since the deeper the understanding, the more effective the strategies to fight decoherence can be. Within the context of quantum information processing two prominent examples of strategies against decoherence are quantum error correction and dynamical decoupling [2]. However, the application of these schemes is subject to some restrictions (e.g. logical overheads, noise threshold or extremely short pulse timescales) and in general the implementation of a sequence of quantum gates within these approaches remains hard. More flexible methods to counteract noise in such a way to allow quantum computing and in general survival of quantum coherence on

useful timescales are therefore highly desirable. In this respect quantum control theory offers a valuable way to go. The general idea behind quantum control is to use the interaction of a quantum system with a properly tailored classical control field to steer its dynamics towards the desired outcome. In this perspective error correction and dynamical decoupling can be regarded as specific instances of quantum control.

Unfortunately even without considering feedback schemes, when it comes to open systems, quantum control is still a mathematically challenging subject. Indeed although substantial progress has been recently made [3, 4] to develop an general framework, only very simple models have been solved so far. Our goal is to study a more rich system by tackling the problem *already before the derivation of a reduced dynamics*. That is, we study the control system before the infamous "bath trace" is performed and then conclude on the control properties of the open system. The problem with this approach is that, for infinite baths, it requires the investigation of the control properties of infinite dimensional systems which is almost equally challenging as that of open systems. We have therefore decided to examine the spin-star model [5, 6, 7, 8], where a central spin interacts with a finite set of surrounding environmental spins. The spin star represents a finite but scalable system, so that in principle the thermodynamic limit can be looked at, and even for small environment sizes it is already experimentally relevant because it can be used to describe the main sources of decoherence in NV centers [9, 10, 11, 12] and quantum dots [13, 14, 15]. In addition the spin star model has been subject to a series of studies concerning its reduced dynamics, so there is hope to bring the two aforementioned research lines together on a practically relevant system. In the present paper, we go in this direction by considering a spin bath controlled through the central system, and completely characterizing the theoretical control properties of both the bath and the central system.

2. The model

We consider a spin-star set up consisting of a central spin surrounded by N spins as shown in Fig.1. The spins surrounding the central spin will be hereafter referred to as the *bath* spins keeping in mind that, strictly speaking, they represent a true spin bath only in the thermodynamic limit. We assume that the central spin interacts with the bath spins via an isotropic Heisenberg interaction and that it is additionally subject to a constant magnetic field. The model is thus described by the following Hamiltonian

$$H_0 = \sigma_y + \sum_{k=1}^N A_k \boldsymbol{\sigma} \cdot \boldsymbol{\sigma}^{(k)}, \quad (1)$$

where A_k is the coupling between the central and the k th bath spin, and $\boldsymbol{\sigma} = (\sigma_x, \sigma_y, \sigma_z)$ and $\boldsymbol{\sigma}^{(k)} = (\sigma_x^{(k)}, \sigma_y^{(k)}, \sigma_z^{(k)})^T$ are the Pauli matrices acting on the central and the k th bath spin respectively. Due to the isotropy of the Heisenberg interaction, the specific choice of σ_y as the central spin Hamiltonian does not represent a loss of generality. Under the assumption of equal system-bath couplings, i.e. $A_k = A$ for each k , the

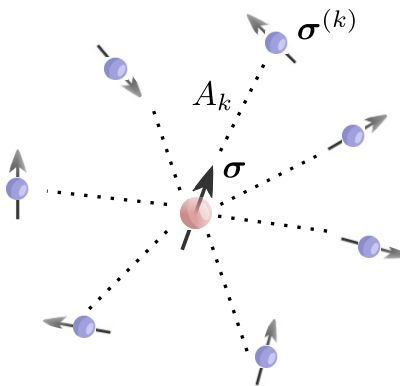


Figure 1. The model described by Hamiltonian (1): a central spin described by σ interacts via an isotropic Heisenberg interaction with N surrounding spins each described by $\sigma^{(k)}$. The coupling between the system and the k th bath spin is given by A_k . The central spin interacts additionally with a classical control field as described by the Hamiltonian (4).

dynamics of the central spin and the entanglement properties of similar models have been studied analytically in [5, 6, 7] by means of a non-Markovian master equation. If all couplings are equal, in fact, the Hamiltonian (1) can be rewritten as a two-particle Hamiltonian

$$H_0 = i(\sigma_- - \sigma_+) + 2A(\sigma_- J_+ + \sigma_+ J_- + \sigma_z J_z), \quad (2)$$

where $\sigma_{\pm} = (\sigma_x \pm i\sigma_y)/2$ are the lowering and raising operators acting on the central spin and the bath is regarded as a single effective particle with angular momentum operator

$$\mathbf{J} = \frac{1}{2} \sum_{k=1}^N \sigma^{(k)}, \quad (3)$$

and corresponding raising and lowering operators given by $J_{\pm} = J_x \pm iJ_y$. The Hamiltonian (2) conserves the square of the bath angular momentum, i.e. $[\mathbf{J}^2, H_0] = 0$. Hence, noting $[J_z, \mathbf{J}^2] = 0$, simultaneous eigenstates of \mathbf{J}^2 and J_z represent a convenient basis for the bath. However, since the operators \mathbf{J}^2 and J_z alone do not form a complete set of commuting observables, the subspaces defined by their eigenvalues, denoted by j and m respectively, are not in general one-dimensional. We therefore introduce an additional quantum number ν corresponding to the eigenvalues of certain permutation operators acting on the bath spins and commuting with H_0 . The permutation operators do not need to be specified as the controllability analysis is independent of them. Due to the conservation of j and ν , the bath Hilbert space can be written as a direct sum of the subspaces $\mathcal{H}_{j,\nu}$ and the total Hilbert space can be written as $\mathcal{H} = \mathcal{H}_S \otimes (\bigoplus_{j,\nu} \mathcal{H}_{j,\nu})$ where \mathcal{H}_S is the Hilbert space of the central spin. This Hilbert space structure, as detailed in the following section, lies at the heart of the spin-star controllability properties in the equal coupling scenario.

Having defined the model Hamiltonian H_0 , we now move on to introduce controls. As discussed in the introduction, we assume that only the central spin can be accessed

to and controlled. In order to obtain non-trivial dynamics, the control field acting on the central spin must not commute with H_0 . A convenient choice is therefore represented by a classical magnetic field $B(t)$ along the z direction as described by the control Hamiltonian

$$H_c(t) = B(t)\sigma_z. \quad (4)$$

The full Hamiltonian is thus

$$H(t) = H_0 + H_c(t). \quad (5)$$

Despite representing quite an extreme simplification, still the spin-star model described by Eq. (1) already captures some relevant features of the spin-bath decoherence processes occurring in solid-state systems used for the implementation of quantum technologies such as nitrogen vacancy centers [9, 10] and quantum dots [13, 14, 15]. Such a system therefore represents an interesting and challenging playground for an investigation of controllability of open systems which can also be of practical relevance.

3. Controllability considerations

We now focus on the investigation of which unitary transformations can be implemented on the spin star, in particular on the central spin, using the control field $B(t)$. The dynamics is governed by the Schrödinger equation for the time evolution operator

$$\dot{U}(t) = -i(H_0 + H_c(t))U(t), \quad U(0) = \mathbf{1}, \quad (6)$$

where the drift Hamiltonian H_0 and the control Hamiltonian H_c are those given in Eqs. (1) and (4). All unitary operations which can be implemented on the system constitute the *reachable set* \mathcal{R} . More precisely \mathcal{R} is defined as the set containing all unitary transformations U which are solution of Eq.(6) for some time $\tau > 0$ and a certain control field $B(t)$ with $t \in [0, \tau]$. The closure $\bar{\mathcal{R}}$ of the reachable set consists of the unitaries which can be achieved with arbitrary high precision. It is equal [16] to the Lie group $e^{\mathcal{L}}$, where $\mathcal{L} = \langle iH_0, iH_c \rangle_{[\cdot, \cdot]}$ is the *dynamical Lie algebra* spanned by real linear combinations and nested commutators of iH_0 and iH_c . The system is said to be fully controllable if the Lie group is equal to the unitary group or, in our case of traceless Hamiltonians, to the special unitary group [17, 18]. To analyze the controllability of the spin star we thus need to calculate the associated dynamical Lie algebra.

Without bath spins, i.e. for $N = 0$, the central spin is fully controllable because $[i\sigma_y, i\sigma_z] = 2i\sigma_x$ and $\mathcal{L} = su(2)$. When $N > 0$ it is no longer obvious whether the central spin is fully controllable or not: on the one hand H_0 is necessary to achieve rotations around the x axis, on the other the interaction with the bath spins introduces noise on the central spin. We will therefore study how the bath influences the controllability of the central spin. The controllability of similar spin star models that consists of an anisotropic interaction of the central spin with the bath spins was studied in [19, 20]. Two classical fields were used to control the central spin and it was shown by using the graph criterion [21] that then the whole system becomes controllable. However this

method is based on finding the eigenstates of the system and therefore it is not applicable for the Hamiltonian (1). Moreover, in this case the controllability of the central spin is trivial, and can in principle be achieved arbitrarily quickly through strong control fields, which means that such models are not relevant in the context of the present study.

In the following we will first consider the case when the central spin couples with the same coupling strength to each bath spin and then the case when the couplings are all different from each other.

3.1. Equal couplings

As discussed in section 2, when the central spin couples to each bath spin with the same strength, the bath spins behave like a collective spin described by the angular momentum operator (3) whose square is conserved. Since the control Hamiltonian (4) acts only on the central spin, this symmetry is conserved also in presence of the control field thus implying that the spin star is not fully controllable (see also [22]). However, by performing repeated commutators of iH_0 and iH_c and taking their real linear combinations, we can obtain the operators $i\sigma_\alpha$, iJ_α and $i\sigma_\alpha J_\beta$ with $\alpha, \beta = x, y, z$ (see Appendix A for details). This implies that the full $su(2)$ algebra acting on the Hilbert space of the central spin is contained in the dynamical Lie algebra regardless of the number of bath spins. The central spin is thus fully controllable even in presence of decoherence or, in other words, the noise induced on the central spin as a result of the interaction with the bath can be effectively switched off. More generally, the dynamical Lie algebra for equal couplings contains all elements of the form (see Appendix A)

$$i\sigma_\alpha(J_+^l J_-^k J_z^s + h.c.), \quad \alpha = x, y, z \quad l, k, s \in \mathbb{N}_0. \quad (7)$$

Equation (7) implies full controllability of the spin star within each subspace $\mathcal{H}_S \otimes (\bigoplus_\nu \mathcal{H}_{j,\nu})$ which can be achieved by properly combining the operators J_+^l and J_-^k in such a way to act only on a given j -subspace. Even without full controllability it is still possible to perform many interesting and practically relevant operations on the spin star such as entangling the central spin with the bath or using the bath as a data bus. Such protocols were recently experimentally demonstrated in [23].

The dimension of the dynamical Lie algebra can be obtained by determining the size of the subspaces of fixed ν [5] as $\dim(\mathcal{L}) = \sum_j ((2(2j+1))^2 - 1)$. For a given N , j can only take the values $j = 1/2, 3/2, \dots, N/2$ when N is odd and $j = 0, 1, \dots, N/2$ when N is even, we obtain

$$\dim(\mathcal{L}) = \begin{cases} \frac{1}{6}(2+N)(9+4N(4+N)), & \text{for } N \text{ even,} \\ \frac{1}{6}(1+N)(3+2N)(7+2N), & \text{for } N \text{ odd,} \end{cases} \quad (8)$$

which shows that the dimension of the dynamical Lie algebra scales polynomially $\propto N^3$ with the size of the bath.

3.2. Different couplings

In the previous section we learned that in the equal-coupling case the central spin is fully controllable but, due to the symmetries of the system, the whole spin star is not. The situation changes if all coupling constants A_k are different from one another. In this case the system has no more symmetries and the bath spins do not behave like a collective spin anymore. Full controllability of the central spin still holds for almost all choices of the coupling constants and is independent of both the size and the initial state of the bath, see (Appendix B.1). In addition each single bath spin is fully controllable, see (Appendix B.2), thus allowing us to write

$$\sigma_\alpha^{(k)} \in \mathcal{L}, \quad \forall k = 1, \dots, N, \quad \alpha = x, y, z. \quad (9)$$

Hence, due to the Heisenberg interaction between the central and the bath spins, full controllability of the spin star $\mathcal{L} = su(2^{N+1})$ is achieved [25]. As a consequence, the dimension of the dynamical Lie algebra scales exponentially with the bath size. By acting with a control field on the central spin alone all degrees of freedom, even the inaccessible ones, can be used for quantum information tasks.

3.3. Implementing CPT maps

An interesting generalization of the above is to consider the ability to implement completely positive trace preserving (CPT) maps on the central system. This is especially relevant in view of the growing interest towards open quantum system simulators [26, 27, 28, 29] and quantum reservoir engineering [30, 31]. We find that arbitrary CPT maps $\mathcal{D}(\rho_S)$ can be implemented: first, let us consider the unequal coupling case with $N \geq 2$. We initialize two spins of the bath in a pure state ϕ_B through consecutive unitary operations and measurements on the central spin. Using controls we then implement the unitary U of the Stinespring representation $\mathcal{D}(\rho_S) = \text{tr}_{12} \{U(\rho_S \otimes \phi_B)U^\dagger\}$ of \mathcal{D} , and thus \mathcal{D} . Second, for equal couplings even though the whole system is not fully controllable it is still possible to implement every unitary operation within the subspaces $\mathcal{H}_S \otimes (\bigoplus_\nu \mathcal{H}_{j,\nu})$. Provided they are large enough ($j > 3/2$, implying $N > 3$) and provided the bath can be initialized appropriately, we can again implement a Stinespring dilation of \mathcal{D} .

3.4. Numerical calculation of the dynamical Lie algebra

In this section we will examine more in detail the structure of the dynamical Lie algebra, \mathcal{L} , using a numerical algorithm similar to those discussed in [32] and [33]. In order to obtain a complete operator basis for \mathcal{L} it is enough to repeatedly compute the commutators with iH_0 and iH_c , until the rank of \mathcal{L} does not increase any further [33]. Such a procedure can be visualized as a tree, the so-called Lie tree. Indeed in Fig. 2 we show the Lie tree of a spin star with $N = 2$ bath spins for both equal, a), and different, b), couplings. The numbers inside the circles label the elements of \mathcal{L} starting with iH_c and iH_0 which correspond to 1 and 2. The blue/red branches indicate that

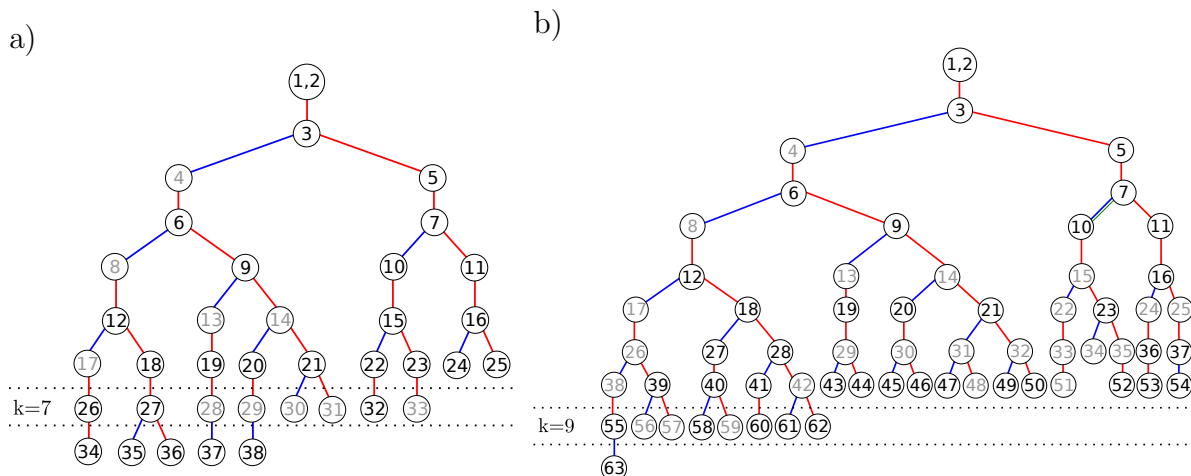


Figure 2. Tree structure of the dynamical Lie algebra for $N = 2$ bath spins and either equal (a) or different (b) couplings. The numbers in the circles represent the elements of the dynamical Lie algebra and the branches indicate whether the new linearly independent term was obtained by commutation with iH_c (blue) or iH_0 (red). The index k indicates the depth of the commutator. Numbers in gray denote the elements which, by real linear combinations, give $i\sigma_x$ on the central spin such that the central spin is fully controllable.

the new element was obtained by commutation with iH_c/iH_0 respectively. The number k denotes the depth of the tree nodes starting with $k = 1$ for $[iH_c, iH_0]$. More generally, we define the depth of an element of \mathcal{L} as the maximal depth of nodes required to express it via linear combinations. Although the tree structure is not unique, because it depends on the order according to which commutators are performed, using the Jacobi identity it can be shown that the depth of an element is independent of the specific tree structure. To achieve full controllability of the central spin the crucial element to be obtained is $i\sigma_x$. In order to determine its depth, we highlight nodes corresponding to the basis elements that are needed to construct it in gray.

By comparing panels a) and b) of Fig. 2, where the depth of σ_x is $k = 7$ and $k = 9$ respectively, we can conclude that the value of the couplings, i.e. the presence of symmetries of the drift Hamiltonian, affects the depth at which full controllability of the central spin is achieved. In both cases the tree structure is rather rich which is reflected by the complex proof of the central-spin full controllability presented in the appendix.

In the equal coupling case the depth of $i\sigma_x$ is upper bounded by 24 since it can be obtained in fashion independent of the bath size (see Appendix A). In contrast, for different couplings, the depth of $i\sigma_x$ in the proof Appendix B.1 indicates a linear scaling with the bath size. However, this only represents an upper bound on the scaling because a different proof might exist yielding a lower depth. By considering a perturbation expansion of the time-evolution operator, it is tempting to conjecture that the depth of an element of the dynamical Lie algebra is related to the minimum time required to achieve its unitary companion. Unfortunately we do not have enough numerical data

to decide this conjecture and leave it as an open problem for future studies.

4. Influence of the bath on the minimum gate time

So far we have discussed which unitary transformations can be implemented *in principle* on the spin star by a generic control field $B(t)$. By this we mean that no explicit statement is made about the time required to achieve the desired unitary. In practice, we not only need to reach the desired unitary but we need to do so in a reasonable time. Therefore we now turn to the question of how the minimum time, $T^*(U_G)$, required to implement a target unitary transformation, U_G , on the central spin (hereafter minimum gate time) scales with the number of bath spins. To do this we need to identify the control pulse allowing to implement U_G in the shortest time possible for different numbers of bath spins. To this end we need to resort to numerical gate optimization.

We used the Grape algorithm [34] as implemented in the open source optimal control package DYNAMO [35]. A detailed explanation of the algorithm and the package can be found in [36]. The algorithm uses a gradient based method that maximizes the following gate fidelity

$$f_1(\tau) = \left| \frac{1}{2^{N+1}} \text{tr}\{U_G^\dagger U(\tau)\} \right|^2, \quad (10)$$

given by the modulus square of the normalized overlap, at a given time τ , between the target transformation, U_G , and the actual evolution, U . The fidelity (10) involves choosing a target unitary operation acting on the whole spin star. However, since we are interested in implementing unitary transformations on the central spin alone (and in general we cannot access the bath degrees of freedom), such a choice is somewhat arbitrary and limiting. In an open system set up a better and more motivated fidelity measure is therefore given by [37]

$$f_2(\tau) = 1 - \lambda \min_V \|U_G \otimes V - U(\tau)\|^2, \quad (11)$$

where U_G is the target unitary on the central system, V a generic unitary on the bath, U is the actual evolution at time τ of the full system and λ is a normalization constant. Due to the minimization over all the unitaries acting on the bath, as opposed to the fidelity in Eq. (10), the fidelity defined in Eq. (11), reaches its maximum if the goal transformation has been implemented on the central system regardless of the bath evolution. Using the Frobenius norm and choosing $\lambda = 1/(2 * 2^{N+1})$, the minimization can be carried out explicitly yielding [38]

$$f_2(\tau) = \frac{1}{2^{N+1}} \text{tr}\{\sqrt{Q^\dagger Q}\}, \quad (12)$$

with $Q = \text{tr}_S\{(U_G \otimes \mathbb{1}_{\text{bath}})^\dagger U(\tau)\}$, and tr_S the partial trace over the central spin degrees of freedom.

After having included the gate fidelity f_2 into the DYNAMO package, we have performed the optimization of f_1 and f_2 by using the exact gradient formula developed in [38, 39]. The time τ , from now on called the driving time, has been divided into M

equidistant time intervals $\Delta t = 0,05$ chosen to be smaller than the inverse of the highest eigenvalue of the Hamiltonian (1) to ensure a proper resolution of the dynamics. For a given bath size, in order to estimate the minimum gate time T^* , we have optimized both figures of merit $f_1(\tau)$ and $f_2(\tau)$ for different values of τ . We additionally optimized over randomly chosen initial pulses meaning that at each τ the maximum value of the fidelity over the different realizations is taken. An additional optimization over many initial pulses is performed to minimize the effect of local minima in the numerical routine. Additionally, to ensure the existence of the thermodynamic limit we have rescaled the coupling constants A_k by a factor $\frac{A_k}{\sqrt{N}}$ [7].

We emphasize that our numerical calculations can only provide upper bounds to the minimum gate time, because the choice of initial control field can affect the time at which the given fidelity reaches a predetermined threshold value.

4.1. Optimizing f_1

We begin with the optimization of the fidelity $f_1(\tau)$ defined in Eq. (10) and choose the identity as the target unitary on the bath. As a target transformation U_G on the central system we consider both the Hadamard gate and the $\pi/8$ gate since these one-qubit gates form a universal set [40]. We begin with equal couplings, set $A = 1$, and investigate the minimum time required for the implementation of the Hadamard gate (Fig. 3 panel *a*) and the $\pi/8$ gate (Fig. 3 panel *b*) on the central spin. In Fig. 3 we plot the maximum value of $f_1(\tau)$ as a function of the driving time τ for different number of bath spins N and maximized over 200 randomly chosen initial pulses. Points that seem to break the continuity of the curves are statistical fluctuations and have no physical relevance as confirmed by optimizations over a higher number of initial pulses. The computational effort required by the optimizations is intensive which is the reason why, when optimizing f_1 , we restricted ourselves to a statistical sample of 200 random initial pulses for each time and, when optimizing f_2 , to 500. The black curve corresponds to $N = 0$ whereas the other curves to increasing values of N : in panel *a*) $N = 1, \dots, 7$ and in panel *b*) $N = 1, \dots, 5$. We observe the following:

1) *Short time behavior in the equal coupling case:* for $\tau = 0$ we have obtained $f_1(0) = 0$ for the Hadamard gate and $f_1(0) = (2 + \sqrt{2})/4$ for the $\pi/8$ gate. The plots show the bath detrimental effect on gate optimization on short time scales. Indeed after an initial extremely short time window where all curves exhibit the same increasing behaviour, reflecting the fact that correlations between the central system and the bath have not been established yet, the maximum value of the fidelities in presence of the spin bath then drops compared to the $N = 0$ case. Note that for short times the $\pi/8$ gate can be reached with fidelities above 0.99 independently of the number of bath spins. This reflects the fact that the $\pi/8$ gate is up to a global phase identical to a rotation around the z axis which can always be achieved at short times with a sufficiently large control-field amplitude.

2) *Long time behavior in the equal coupling case:* after a region of decreasing slope,

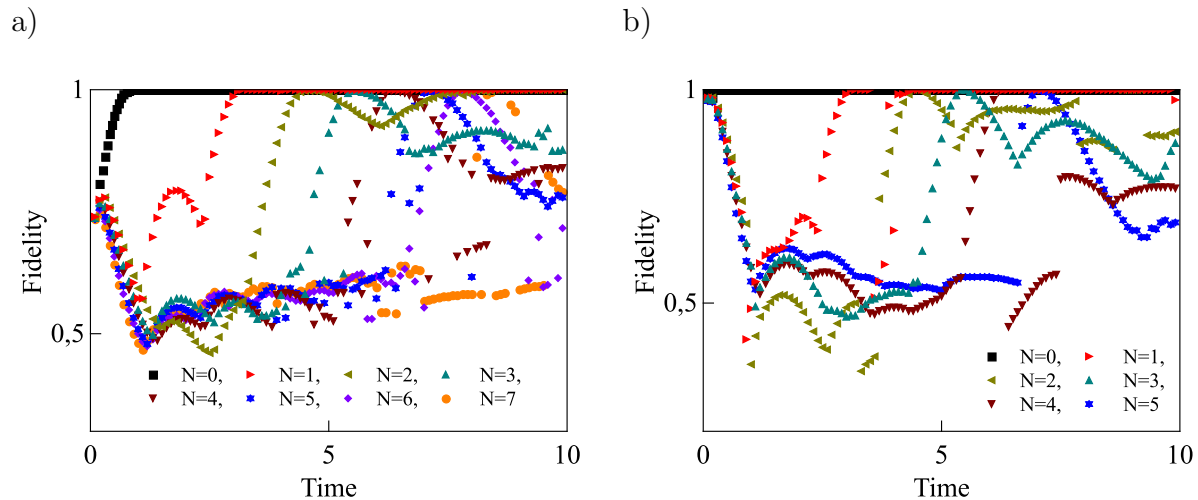


Figure 3. Maximum value of the fidelity $f_1(\tau)$ as a function of the driving time τ extracted from 200 random initial pulses for equal couplings and target unitary *a*) Hadamard on the central spin and identity on the bath; *b*) $\pi/8$ on the central spin and identity on the bath. Both plots have been obtained for different numbers N of bath spins as indicated on the figure.

all dissipative fidelities increase again until, for all N , a maximum value above 0.995 is reached. The increasing bath size results in a time shift of the maximum value. The achieved maximum values are the same for both the Hadamard and the $\pi/8$ gate.

3) Different coupling case: to study the effect of the bath spins in more detail we will from now on focus only on the optimization of the Hadamard gate on the central spin. Figure 4 shows the maximum value of the fidelity as a function of the driving time in the different coupling case. The couplings are randomly chosen from a uniform distribution between 1 and 2. The curves have been obtained for $N = 1, \dots, 3$ bath spins. As before, a maximum value above 0.995 is reached for all bath sizes but the driving time needed to reach it is much longer with respect to the equal coupling case.

4) Estimation of T^ :* in Fig. 5 we plot the estimated minimum gate time T^* against the number of bath spins for different and equal couplings. Our estimate has been obtained by setting a threshold value for the fidelity $f_1 = 0.995$ and extracting the corresponding T^* from the data plotted in Fig. 3 and 4. The inset shows the minimum gate time versus the number of bath spins for different couplings on a logarithmic scale. It should be mentioned here that the point that belongs to $N = 4$ for different couplings was obtained by searching only in the expected time window for a fidelity above the mentioned threshold. Furthermore, as already mentioned, our results can only provide an upper bound on T^* . Nevertheless Fig. 5 clearly suggests a significantly different scaling behaviour of the minimum gate time in the two different coupling regimes. In the equal coupling case, when the whole system is not fully controllable, the gate time seems to depend weakly on the number of bath spins (red curve) in strong contrast with the fully controllable case (black curve) where the dependence on the bath size is at least polynomial (black curve). Consistently with our controllability analysis, the scaling

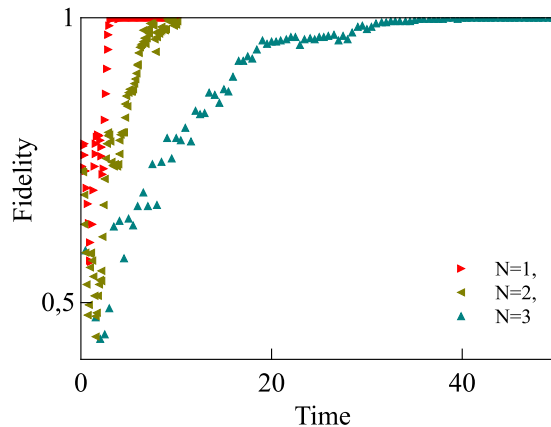


Figure 4. Maximum value of the fidelity $f_1(\tau)$ as a function of the driving time τ extracted from 200 random initial pulses for different couplings and bath size $N = 1, \dots, 3$.

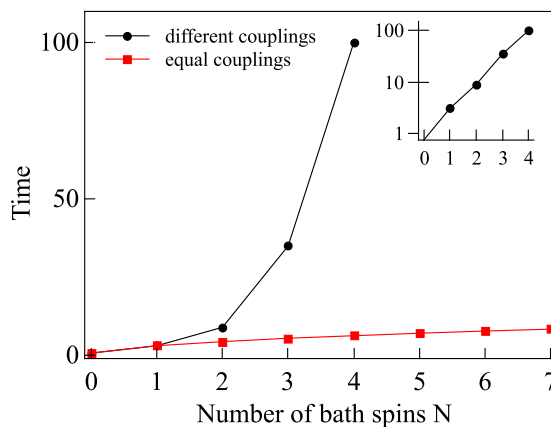


Figure 5. Minimum gate time T^* needed to reach a value of the fidelity of at least $f_1(\tau) = 0.995$ as a function of the number of bath spins N for both different and equal couplings. The inset shows the curve for different couplings on a logarithmic scale.

of the minimum gate time suggests that in the equal coupling case the decoherence affecting the central spin can be suppressed in reasonable time regardless of the size of the bath. On the other hand, in the fully controllable case, for higher number of bath spins (dramatically) longer gate times can be expected. This seems consistent with the intuition that if the dimension of the Lie Algebra grows exponentially with N , then the implementation of a generic element of the corresponding Lie group requires an exponentially increasing time.

4.2. Optimizing f_2

Until now we have investigated the scaling of the minimum gate time by optimizing f_1 and choosing the identity as a target operation on the bath. We now want to see whether

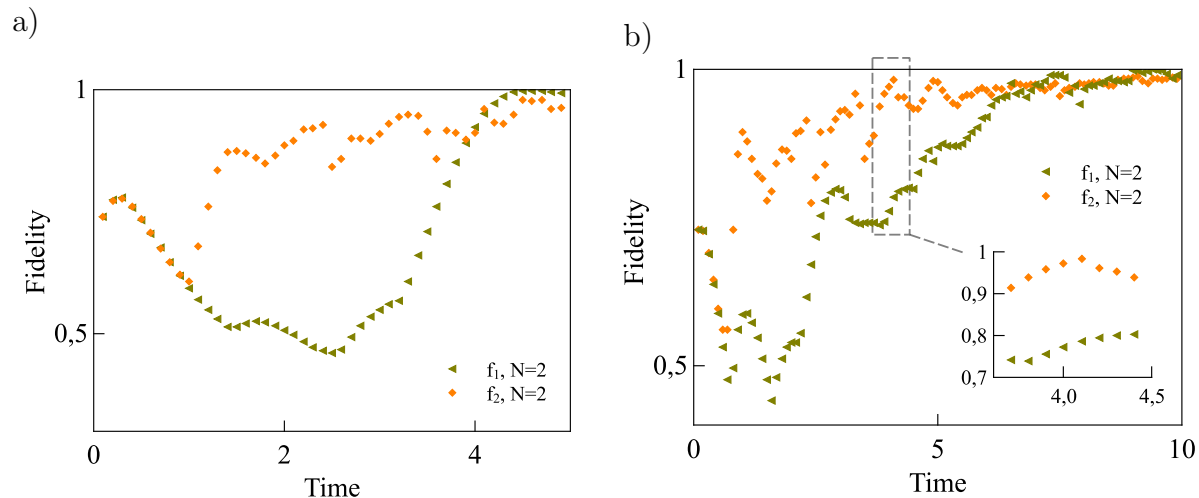


Figure 6. Maximum values of the fidelities $f_1(\tau)$ and $f_2(\tau)$ as a function of the driving time τ extracted from 500 randomly chosen initial pulses for $N = 2$: a) equal couplings, b) different couplings where the inset shows the time window $\tau \in [3.7, 4.4]$ and the maximum was extracted from 10^4 random initial pulses.

the optimization of f_2 , Eq. (12) exhibits significant deviations from this behaviour. Unfortunately the optimization of f_2 with the GRAPE algorithm resulted extremely sensitive to local minima, especially for increasing number of bath spins, consistently also with the results presented in [38]. In order to minimize this effect a much higher number of random initial pulses was required. Due to computational restrictions, we had therefore to limit our investigation to $N = 2$ and 500 random initial pulses.

In Fig.6 the maximum value of the fidelities $f_1(\tau)$ (dark yellow curve) and $f_2(\tau)$ (orange curve) is plotted as a function of the driving time τ for both equal (panel a)) and different couplings (panel b)). Intuitively we would expect a shorter minimum gate time when the target transformation is specified only on the central spin because in this case the constraint on the bath evolution is weaker. Each control pulse maximizing $f_1(\tau)$ is a specific solution for $f_2(\tau)$ as well, hence the fidelity $f_2(\tau)$ should at least attain the same maximum values as $f_1(\tau)$. However, from Fig.6, we see that values of the maxima reached by f_2 around T^* are slightly below those reached by f_1 thus witnessing an increased sensitivity of the optimization to local minima within this time window. From Fig.6 we also note that up to a certain time τ the curves relative to $f_2(\tau)$ and $f_1(\tau)$ are identical, thus implying that within this time window there is no difference between setting the target on the full system or on the central spin only. This behavior however changes at increasing times since higher fidelities can be achieved on shorter timescales if the target is only set on the central spin. Only at the end of the time window the curves seems to become similar again. However, for equal couplings, even though f_2 reaches higher values at shorter times, it never crosses the threshold of $f_2 = 0.995$ before T^* thus leading us to conclude that in this case, for sufficiently high threshold values, the fidelity used does not significantly affect the estimate of the upper bound on the minimum gate time. For different couplings, instead, values that are close to the

threshold can be reached at short times: the inset plot shows a time window in which $f_2(\tau)$ reaches a maximal value of 0.98.

In conclusion, for equal couplings, the numerical results suggest that the minimum gate time depends weakly on the size of the bath and perhaps reaches a saturation value. This is consistent to the theoretical prediction that the depth of an element of the dynamical Lie algebra is related to the minimum gate time to achieve its unitary companion (see section 3.4). This behavior appears to be the same for both fidelities. For different couplings, instead, the numerical results hint at a different behaviour of the minimum gate time according to whether the target is defined on the whole system or on the central spin only. In the latter case in fact not only the minimum gate time seems to be shorter but also we can not even rule out the possibility that it scales as in the equal coupling case. More conclusive statements require much bigger computational resources and more sophisticated analytical techniques as for example those suggested in [41, 42]. However these methods are not easily generalized to the high dimensional systems considered here.

5. Conclusions

By analytical calculation of the dynamical Lie algebra, we showed that a central spin interacting with a surrounding spin bath is fully controllable for almost all choices of the coupling constants and any bath size. If the central spin couples to the bath with unequal couplings, this property extends to the whole spin star, environmental spins included. We can therefore conclude that quite remarkably, by controlling the central system, the bath can be i) effectively switched off; ii) arbitrarily engineered. The possibility of controlling the environment via the central spin can be exploited to implement, on the central spin itself, not only arbitrary unitaries but, more generally, arbitrary (completely positive trace preserving) dynamical maps. This result can be of practical relevance both for quantum simulations of open system and for quantum reservoir engineering.

Alongside these purely analytical findings we also performed an extensive numerical investigation of control timescales and how these are affected by both the bath size and the symmetries of the system. In the maximally symmetric scenario, when all the bath spins can be regarded as a single collective particle, our estimate for the minimum time required to perform a gate under dissipative dynamics shows that it scales relatively slow, perhaps reaching a saturation value, as a function of the bath size. On the contrary, in absence of symmetries, i.e. when each environmental spin interacts differently with the central system, the scaling of the minimum gate time appears to be much faster (we conjecture exponentially faster).

Our results might have interesting applications in NV centers, which are essentially electron spins in a finite nuclear spin bath. One recently demonstrated method to overcome the short coherence time of the electron spin is to store its state in the nuclear spins, which have longer decoherence times. Our control results then suggest that this

might not be the best strategy, and that instead one might apply a more complex shaped pulse to the electron spin to keep it fresh for longer.

Acknowledgments

The authors acknowledge fruitful discussions with Sophie Schirmer, Shai Machnes, Thomas Schulte-Herbrüggen and Hubert de Guise. C. Arenz acknowledges financial support through the Eleanor James Scholarship and the Aberystwyth Doctoral Career Development Scholarship. G. Gualdi acknowledges financial support from MIUR through the PRIN grant 2010LLKJBX, from QYMRU, and through the IMAPS summer fellowship. QSTAR is the MPQ, LENS, IIT, UniFi Joint Center for Quantum Science and Technology. G. Gualdi and D. Burgarth want to thank the KITP for support in part by the National Science Foundation under Grant No. NSF PHY11-25915. We acknowledge the DYNAMO code [35].

Appendix A. Lie algebra for equal couplings

First we want to show that $i\sigma_x \in \mathcal{L}$ where we define $A_1 \equiv iH_0$ and $A_2 \equiv iH_c$.

Building the double commutator $[A_2, [A_1, A_2]]$ we get up to a constant the element

$$A_3 = i(\sigma_y + \sigma_+ J_- + \sigma_- J_+), \quad (\text{A.1})$$

which leads with $A_1 - A_3$ to

$$A_4 = i\sigma_z J_z. \quad (\text{A.2})$$

After calculating $[[A_1, A_2], A_3]$ and using the properties of J_- and J_+ we find up to a constant the element

$$A_5 = \sigma_z(J_- - J_+) - 2i\sigma_z(\vec{J}^2 - J_z^2 - J_z) + i\sigma_- \sigma_+ J_z. \quad (\text{A.3})$$

The last two terms of A_5 commute with A_4 and therefore $[A_4, A_5]$ yields, up to a constant

$$A_6 = iJ_x. \quad (\text{A.4})$$

By commuting A_6 with $[A_1, A_2]$ we find $i\sigma_x J_z$ and by commuting with A_2, A_4, A_6 we obtain the following elements

$$\begin{aligned} & i\sigma_z, i\sigma_x J_z, i\sigma_y J_z, i\sigma_z J_z, \\ & iJ_x, i\sigma_x J_y, i\sigma_y J_y, i\sigma_z J_y, \end{aligned} \quad (\text{A.5})$$

which can be used to isolate

$$A_7 = i(\sigma_y + \sigma_x J_x), \quad (\text{A.6})$$

from A_1 . By commuting A_7 with $i\sigma_x J_z$ we obtain iJ_y and the commutator $[i\sigma_x J_z, iJ_y]$ yields up to a constant $i\sigma_x J_x$ which can be used, together with A_7 , to reach $i\sigma_y$. We then also have $i\sigma_x$ by using A_2 . In fact we showed that

$$i\sigma_\alpha, iJ_\beta, i\sigma_\alpha J_\beta \in \mathcal{L}, \quad \forall \alpha, \beta = x, y, z. \quad (\text{A.7})$$

Due to the fact that the ladder operators σ_{\pm} and J_{\pm} define another representation it is easy to verify that $i(\sigma_{\alpha}J_{\beta} + h.c.) \in \mathcal{L}$ holds also for $\alpha, \beta = \pm, z$.

With the elements we found so far we can find other elements by building their commutators and creating real linear combinations. Next we show that

$$i\sigma_{\alpha}(J_{+}^l J_{-}^k J_z^s + h.c.) \in \mathcal{L}, \quad \forall l, k, s \in \mathbb{N}, \quad \alpha = x, y, z. \quad (\text{A.8})$$

Essentially, this characterizes the dynamical Lie algebra up to normal ordering of operators. We will proceed by induction and define

$$A(K) = \text{span}\{i\sigma_{\alpha}(J_{+}^l J_{-}^k J_z^s + h.c.) \mid l + k + s \leq K, \alpha = x, y, z\}, \quad (\text{A.9})$$

where hereafter Greek indices describe some x, y, z for the Pauli spin operators and some \pm, z for the angular momentum operators.

The initial step is to prove that $A(1) \subset \mathcal{L}$. This is trivial because we already have proven with (A.7) that $\{i\sigma_{\alpha}(J_{\beta} + h.c.)\}$ is a subset of \mathcal{L} . We can therefore go to the inductive step and show that if $A(K) \subset \mathcal{L}$ then $A(K+1) \subset \mathcal{L}$.

Take any $a = i\sigma_{\alpha}(J_{+}^l J_{-}^k J_z^s + h.c.) \in A(K+1)$ with $l + k + s = K + 1$ and calculate for $s > 0$ the commutator

$$\begin{aligned} & [i\sigma_{\alpha}(J_{+}^l J_{-}^k J_z^{s-1} + h.c.), i\sigma_{\beta}J_z] = \\ & \sigma_{\beta}\sigma_{\alpha}(J_z J_{+}^l J_{-}^k J_z^{s-1} + J_z^s J_{+}^k J_{-}^l) - \sigma_{\alpha}\sigma_{\beta}(J_{+}^l J_{-}^k J_z^s + J_z^{s-1} J_{+}^k J_{-}^l J_z), \end{aligned} \quad (\text{A.10})$$

keeping in mind that if $i\sigma_{\alpha}(J_{+}^l J_{-}^k J_z^{s-1} + h.c.) \in A(K)$ then the above commutator is by construction an element of \mathcal{L} . Due to the anticommutation rules of the Pauli spin operators, we can always choose a σ_{β} so to obtain from Eq. (A.10) up to a constant the following

$$[i\sigma_{\alpha}(J_{+}^l J_{-}^k J_z^{s-1} + h.c.), i\sigma_{\beta}J_z] = a + O, \quad (\text{A.11})$$

with $O \in A(K)$. The cases $l > 0$ and $k > 0$ can be treated analogously and therefore we showed that $a \in \mathcal{L}$, $\forall l, k, s \in \mathbb{N}$. \square

Appendix B. Controllability proofs

Appendix B.1. Controllability of the central spin

In this section we will prove controllability of the central spin by using the determinant of a Vandermonde matrix along the lines of [24]. We want to prove that $su(2) \subset \mathcal{L}$, $\forall N \in \mathbb{N}$ for almost all values of the couplings constants A_k . By $su(2)$ we denote the special unitary algebra acting on the central spin. To be as general as possible we rewrite the system Hamiltonian (1) as

$$H_0 = \sigma_y + \sum_{n=1}^{\tilde{N}} h_n (\sigma_x J_x^{(n)} + \sigma_y J_y^{(n)} + \sigma_z J_z^{(n)}), \quad (\text{B.1})$$

where each set n of bath spins with identical A_k 's are combined as collective particles, coupled to the central system with strength h_n and with corresponding angular momentum operators $J_{\alpha}^{(n)}$ with $\alpha = x, y, z$. We assume that $|h_n| \neq |h_m|$ and

$|h_n - h_m| \neq |h_i - h_j|$ with $(n, m) \neq (i, j) \neq (j, i)$. In general these assumptions are only instrumental to the analytical proof and have neither physical meaning nor are necessary in practice as witnessed by numerical calculations of the dimension of the dynamical Lie algebra. An exception occurs for the full controllability of the whole spin star. In this instance, which will be discussed later in Appendix B.2, both the analytical proof and the numerical calculations show that the assumption $|h_n| \neq |h_m|$ is necessary. In order to prove full controllability of the central spin, we need to prove that the operator $i\sigma_x$ acting on the central spin belongs to the dynamical Lie algebra \mathcal{L} . To this end we begin by commuting iH_0 with the control Hamiltonian (4) and get by real linear combinations the elements

$$B_1 = i(\sigma_y + \sum_{n=1}^{\tilde{N}} h_n(\sigma_x J_x^{(n)} + \sigma_y J_y^{(n)})), \quad (\text{B.2})$$

$$B_2 = i\sigma_z \sum_{n=1}^{\tilde{N}} h_n J_z^{(n)}, \quad (\text{B.3})$$

$$B_3 = i(\sigma_x + \sum_{n=1}^{\tilde{N}} h_n(\sigma_x J_y^{(n)} - \sigma_y J_x^{(n)})). \quad (\text{B.4})$$

We can now observe that proving $i\sigma_x \in \mathcal{L}$ amounts to prove that $iJ_x^{(i)} \in \mathcal{L}$. Indeed $i\sigma_x$ is obtained by performing commutators of $iJ_x^{(i)}$ and B_1, B_2, B_3 and real linear combinations of the resulting elements. The double commutator $[[B_1, B_3], B_2]$ yields up to a constant the element

$$B_4 = i\left(\sum_{n=1}^{\tilde{N}} h_n^2 J_x^{(n)} + \sum_{n>m=1}^{\tilde{N}} (h_n - h_m)h_n h_m (J_x^{(n)} J_y^{(m)} - J_x^{(m)} J_y^{(n)})\right). \quad (\text{B.5})$$

At this point the key observation is that up to a constant

$$\begin{aligned} & \sum_{n>m=1}^{\tilde{N}} c_{n,m} [[(J_x^{(n)} J_y^{(m)} - J_x^{(m)} J_y^{(n)}), B_2], B_2] \\ &= \sum_{n>m=1}^{\tilde{N}} (h_n - h_m)^2 c_{n,m} (J_x^{(n)} J_y^{(m)} - J_x^{(m)} J_y^{(n)}), \end{aligned} \quad (\text{B.6})$$

and

$$\sum_{n=1}^{\tilde{N}} d_n [[J_x^{(n)}, B_2], B_2] = \sum_{n=1}^{\tilde{N}} h_n^2 d_n J_x^{(n)}, \quad (\text{B.7})$$

with $c_{n,m}$ and d_n some coefficients. Using the operator B_4 and Eqs. (B.6) and (B.7), we can create operators of the form

$$B^{(s)} = i\left(\sum_{n=1}^{\tilde{N}} h_n^{2(s+1)} J_x^{(n)}\right)$$

$$+ \sum_{n>m=1}^{\tilde{N}} (h_n - h_m)^{2s+1} h_n h_m (J_x^{(n)} J_y^{(m)} - J_x^{(m)} J_y^{(n)}), \quad (\text{B.8})$$

with $B^{(0)} = B_4$, $[[B^{(s)}, B_2], B_2] = B^{(s+1)}$ and $s = 0, \dots, \tilde{N} - 1$.

We now need to show that the operators of the kind $X^{(s)} \equiv \sum_{n=1}^{\tilde{N}} h_n^{2(s+1)} J_x^{(n)}$ contained in each $B^{(s)}$, Eq. (B.8), are all linearly independent. In fact, if all $X^{(s)}$ are linearly independent then the determinant of the matrix corresponding to the linear set of equations

$$\begin{pmatrix} h_1^2 & h_2^2 & \cdots & h_{\tilde{N}}^2 \\ h_1^4 & h_2^4 & \cdots & h_{\tilde{N}}^4 \\ \vdots & \vdots & \ddots & \vdots \\ h_1^{2\tilde{N}} & h_2^{2\tilde{N}} & \cdots & h_{\tilde{N}}^{2\tilde{N}} \end{pmatrix} \begin{pmatrix} J_x^{(1)} \\ J_x^{(2)} \\ \vdots \\ J_x^{(\tilde{N})} \end{pmatrix} = \begin{pmatrix} X^{(0)} \\ X^{(1)} \\ \vdots \\ X^{(\tilde{N}-1)} \end{pmatrix} \quad (\text{B.9})$$

is non-vanishing. We now define $\tilde{h}_n = h_n^2$, divide the columns of the matrix (B.9) by \tilde{h}_n and then transpose. In this way we obtain a Vandermonde matrix whose determinant

$\prod_{1 \leq i < j \leq \tilde{N}} (\tilde{h}_j - \tilde{h}_i)$ is non-vanishing if $|h_j| \neq |h_i|$, $\forall i \neq j$ as assumed in the beginning.

By real linear combination of the operators $B^{(s)}$ the operator

$$\tilde{B}_i = i(J_x^{(i)} + \sum_{n>m=1}^{\tilde{N}} \xi_{n,m}^{(i)} (J_x^{(n)} J_y^{(m)} - J_x^{(m)} J_y^{(n)})), \quad (\text{B.10})$$

can be selected. If all $\xi_{n,m}^{(i)}$ in Eq. (B.10) are zero then we immediately obtain the operator $iJ_x^{(i)}$ as an element of \mathcal{L} . If this is not the case, using Eqs. (B.6) and (B.7) we can again construct s operators of the form

$$\begin{aligned} \chi^{(s)} &= i(h_i^{2s} J_x^{(i)} \\ &+ \sum_{n>m=1}^{\tilde{N}} (h_n - h_m)^{2s} \xi_{n,m}^{(i)} (J_x^{(n)} J_y^{(m)} - J_x^{(m)} J_y^{(n)})) \end{aligned} \quad (\text{B.11})$$

with $s = 1, \dots, (\tilde{N}^2 - \tilde{N})/2$ assuming that all coefficients $\xi_{n,m}^{(i)}$ are different from zero. As before we can associate them to a Vandermonde matrix with non-vanishing determinant provided that $|h_n - h_m| \neq |h_i - h_j|$, $\forall (n, m) \neq (i, j) \neq (j, i)$. By real linear combinations of the $\chi^{(s)}$'s we can then select the operator

$$\tilde{\chi}_{n,m} = i(\lambda J_x^{(i)} + \omega_{n,m} (J_x^{(n)} J_y^{(m)} - J_x^{(m)} J_y^{(n)})). \quad (\text{B.12})$$

If the coefficient λ is zero we can obtain $iJ_x^{(i)}$ by real linear combinations of $\omega_{n,m} (J_x^{(n)} J_y^{(m)} - J_x^{(m)} J_y^{(n)})$ and the B_i 's (B.10). Instead, if $\lambda \neq 0$, using Eqs. (B.6) and (B.7), we can obtain from $\tilde{\chi}_{n,m}$ a second linearly independent operator with the same structure and then, by real linear combination of the two operators, the operator $iJ_x^{(i)}$. Since $iJ_x^{(i)} \in \mathcal{L}$ we have $i\sigma_x \otimes \mathbb{1}_{\text{bath}} \in \mathcal{L}$ and hence the central spin is fully controllable.

Appendix B.2. Full controllability

By commuting $iJ_x^{(i)}$ with B_1 and B_2 and using the full controllability of the central spins we obtain by real linear combinations $iJ_y^{(i)} \in \mathcal{L}$ and hence $iJ_z^{(i)} \in \mathcal{L}$. This implies that each collective particle contained in Eq. (B.1) is fully controllable. If all system-bath coupling constants are different from each other this implies full controllability of each bath spin and due to the Heisenberg interaction with the central spin the Lie algebra is given by $su(2^{N+1})$ [25] meaning that the whole system is fully controllable. We emphasize that controllability of the whole spin star can only be achieved if all coupling constants are different from each other, because in this case the existence of symmetric manifolds is prevented. The numerical calculation of the dimension of the dynamical Lie algebra shows that even the absolute value of the coupling constants has to be different from each other.

References

- [1] H.-P. Breuer and F. Petruccione, *The Theory of Open Quantum Systems*, Oxford University Press, Oxford (2002).
- [2] D. A. Lidar and T. A. Brun, *Quantum Error Correction*, Cambridge University Press, Cambridge (2013).
- [3] C. O’Meara, G. Dirr and T. Schulte-Herbrüggen Automatic Control, IEEE Transactions. **57**, 2050-2056 (2012).
- [4] T. Schulte-Herbrüggen, A. Spörl, Khaneja A. and S. J. Glaser, J. Phys. B **44**, 154013 (2011).
- [5] A. Hutton, and S. Bose, Phys. Rev. A **69**, 042312 (2004).
- [6] H. P. Breuer, D. Burgarth and F. Petruccione, Phys. Rev. B **70**, 045323 (2004).
- [7] J. Fischer and H. P. Breuer, Phys. Rev. A **76**, 052119 (2007).
- [8] A. Napoli, F. Palumbo and A. Messina, The 12th Central European Workshop on Quantum Optics, J. Phys. Conf. Ser. **36**, 154 (2006).
- [9] R. Hanson, F. M. Mendoza, R. J. Epstein and D. D. Awschalom, Phys. Rev. Lett. **97**, 087601 (2006).
- [10] A. Albrecht, A. Reztker, F. Jelezko and M. B. Plenio, New. J. Phys. **15**, 083014 (2013).
- [11] F. Jelezko, T. Gaebel, I. Popa, A. Gruber and J. Wrachtrup, Phys. Rev. Lett. **92**, 076401 (2004).
- [12] M. V. Gurudev Dutt, L. Childress, L. Jiang, E. Togan, J. Maze, F. Jelezko, A. S. Zibrov, P. R. Hemmer and M. D. Lukin, Science, **316**, 1312-1316 (2007).
- [13] L. Ratschbacher, C. Sias, L. Carcagni, J. M. Silver, C. Zipkes and M. Köhl, Phys. Rev. Lett. **110**, 160402 (2013).
- [14] E.M. Kessler, S. Yelin, M. Lukin, J. I. Cirac and G. Giedke, Phys. Rev. Lett. **104**, 143601 (2010).
- [15] M. Warner, S. Din, I. S. Tupitsyn, G. W. Morley, A. M. Stoneham, J. A. Gardener, Z. Wu, A. J. Fisher, S. Heutz, C. W. M. Kay and G. Aeppli, Nature (2013).
- [16] D. D’Allesandro, *Introduction to Quantum Control and Dynamics*, Chapman & Hall, New York (2008).
- [17] H. Sussmann and V. Jurdjevic, J. Diff. Equat **12**, 313 (1972).
- [18] V. Jurdjevic, *Geometric Control Theory*, Cambridge University Press, Cambridge (1997).
- [19] J. S. Hodges, J. C. Yang, C. Ramanathan and D. G. Cory, Phys. Rev. A. **78**, 010303 (2008).
- [20] Y. Zhang, C. A. Ryan, R. Laflamme and J. Baugh, Phys. Rev. Lett. **107**, 170503 (2011).
- [21] C. Altafini, J. Math. Phys. **43**, 2051 (2002).
- [22] R. Zeier and T. Schulte-Herbrüggen, J. Math. Phys. **52**, 113510 (2011).
- [23] P. London, J. Scheuer, J.-M. Cai, I. Schwarz, A. Retzker, M. B. Plenio, M. Katagiri, T. Teraji, S.

- Koizumi, J. Isoya, R. Fischer, L. P. McGuinness, B. Naydenov and F. Jelezko, *Phys. Rev. Lett.* **111**, 067601 (2013).
- [24] F. Albertini and D. D'Alessandro, *Linear Algebra and its Application* **350**, 213-235 (2002).
- [25] D. Burgarth, S. Bose, C. Bruder and V. Giovannetti, *Phys. Rev. A* **79**, 060305 (2009).
- [26] J. T. Barreiro, M. Müller, P. Schindler, D. Nigg, T. Monz, M. Chwalla, M. Heinrich, C. F. Roos, P. Zoller and R. Blatt, *Nature* **470**, 486 (2011).
- [27] B.-H. Liu, Y.-F. Huang, C.-F. Li, G.-C. Guo, E.-M. Laine, H. P. Breuer and J. Piilo, *Nat. Phys.* **7**, 931 (2011).
- [28] P. Haikka, S. McEndoo, G. De Chiara, G. M. Palma and S. Maniscalco, *Phys. Rev. A* **84**, 031602 (2011).
- [29] P. Schindler, D. Nigg, J. T. Barreiro, E. A. Martinez, M. Hennrich, T. Monz, S. Diehl, P. Zoller and R. Blatt, *Nat. Phys.* **9**, 361 (2013).
- [30] J.F. Poyatos, J.I. Cirac and P. Zoller, *Phys. Rev. Lett.* **77**, 4728 (1996).
- [31] F. Verstraete, M. M. Wolf and J. I. Cirac, *Nat. Phys.* **5**, 633 (2009).
- [32] S.G. Schirmer, H. Fu and A.I. Solomon, *Phys. Rev. A* **63**, 063410 (2001).
- [33] D. L. Elliot, *Bilinear Control Systems*, Applied Mathematical Science, Vol. **169**, Springer (2000).
- [34] N. Khaneja, T. Reiss, C. Kehlet, T. Schulte-Herbrüggen and S. J. Glaser, *J. Magn. Reson.* **172**, 296-305 (2005).
- [35] <http://www.tau.ac.il/~quantum/qlib/qlib.html>
- [36] S. Manches, U. Sander, S. J. Glaser, P. de Fouquieres, A. Gruslys, S. G. Schirmer and T. Schulte-Herbrüggen, *Phys. Rev. A* **84**, 022305 (2011).
- [37] M. D. Grace, J. Dominy, R. L. Kosut, C. Brif and H. Rabitz, *New. J. Phys.* **12**, 015001 (2011).
- [38] F. F. Floethe, P. de Fouquieres and S. G. Schirmer, *New. J. Phys.* **14**, 073023 (2012).
- [39] R. Nigmatullin and S. G. Schirmer, *New. J. Phys.* **11**, 105032 (2009).
- [40] M. A. Nielsen and I.L. Chuang, *Quantum Computation and Quantum Information*, Cambridge University Press (2010).
- [41] N. Khaneja, R. Brockett and S. J. Glaser, *Phys. Rev. A.* **63**, 032308 (2001).
- [42] N. Khaneja, S. J. Glaser and R. Brockett, *Phys. Rev. A.* **65**, 032301 (2002).